



Research article

Dynamic analysis of a phytoplankton-fish model with the impulsive feedback control depending on the fish density and its changing rate

Huidong Cheng^{1,2,*}, Hui Xu² and Jingli Fu^{1,3}

¹ College of Information and Control Engineering, Shandong Foreign Affairs Vocational University, Weihai 264504, China

² College of Mathematics and System Sciences, Shandong University of Science and Technology, Qingdao 266590, China

³ Institute of Mathematical Physics, Zhejiang Sci-Tech University, Hangzhou 310018, China

* **Correspondence:** Email: chd900517@sdust.edu.cn.

Abstract: This paper proposes and studies a comprehensive control model that considers fish population density and its current growth rate, providing new ideas for fishing strategies. First, we established a phytoplankton-fish model with state-impulse feedback control based on fish density and rate of change. Secondly, the complex phase sets and impulse sets of the model are divided into three cases, then the Poincaré map of the model is defined and its complex dynamic properties are deeply studied. Furthermore, some necessary and sufficient conditions for the global stability of the fixed point (order-1 limit cycle) have been provided even for the Poincaré map. The existence conditions for periodic solutions of order- k ($k \geq 2$) are discussed, and the influence of dynamic thresholds on system dynamics is shown. Dynamic thresholds depend on fish density and rate of change, i.e., the form of control employed is more in line with the evolution of biological populations than in earlier studies. The analytical method presented in this paper also plays an important role in analyzing impulse models with complex phase sets or impulse sets.

Keywords: Poincaré map; current growth rate; population density of fish; impulse feedback control; periodic solution

1. Introduction

Phytoplankton is the primary producer of water, it not only provides natural live bait for fish directly or indirectly, but also is the main producer of dissolved oxygen in water body, which is the basis of water productivity. Its quantity determines the density of herbivorous zooplankton, and also determines the output of herbivorous fish. Therefore, the amount of harvested adult fish yields basically depends

on the phytoplankton density. Fish is not only a beneficial food source for human beings, but also an important economic source for fishermen. So, it is of great significance to study phytoplankton-fish models in Marine ecosystems. For example, the commercially valuable phytoplankton-fish predation model proposed in [1] discusses the impact of different factors on the level of fishery. Recent studies [2–5] suggest that persistent or overfishing of specific fish species may lead to the extinction of this species. This prompted the researchers to conduct a more in-depth study of the dynamic properties of the fish and their harvesting.

The basic mathematical tool for designing impulse control system is impulse differential equation theory. Impulse control is a normal form of control based on impulse differential equations [6]. There are many transient changes in nature, such as pest control, glucose regulation, vaccination, etc. [7–9]. When these situations occur, they are not disordered, they develop and change with regularity. To describe them, scholars put forward the time impulse differential equation [10, 11]. Not all the changes are regular like green tide bursts, there are also some changes that are irregular and not limited by time. Scholars from mathematics put forward the state impulse differential equation model to describe them [12, 13]. In recent years, pulsed semi-continuous dynamical systems are widely used in population dynamics [14, 15]. For example, Zeng et al. [16] generalized the Poincaré-Bendixon theorem for ordinary differential equations, and explored the properties of order-1 periodic solutions of predator-prey models with state feedback control. Chen et al. [17] first proposed the method of applying successor functions to study the dynamical simplicity of semi-continuous dynamical systems. Jiang et al. [18, 19] applied Poincaré map to obtain the existence and stability conditions of the order-1 periodic solution of the impulsive semi-dynamic system. Hou et al. [20] investigated a class of predator-prey models with shelter and nonlinear impulse feedback control using Poincaré map. Due to the importance of pulsed semi-continuous dynamic systems in population, impulsive differential equations have attracted more and more attention in recent years, and have been applied in various fields from population dynamics to chemical regulation systems [21–28].

In previous studies, most existing models only consider population size, rather than population growth rate, when proposing control strategies [29, 30]. Usually, when a population reaches a threshold, the number of organisms released during the pulse is independent of population density. A biological point of view, a fixed threshold cannot be combined with the actual situation of the biological population to determine the control strategy. In reality, there are two situations of population growth: 1) The population density is small, but the rate of change is high, which often occurs in the early stage of population growth; 2) The population density is large, but the rate of change is small. Therefore, the threshold of the model needs to consider both the population density and the rate of change, which is more realistic. In the process of biological population control, it is necessary to comprehensively consider different factors, so that the adopted control method is more in line with the development law of biological populations [31]. Based on the above analysis, this paper proposes and studies a comprehensive control model that comprehensively considers fish population density and its current growth rate, and deeply studies the complex dynamic properties of the model, showing the impact of dynamic thresholds on system dynamics.

The rest of this article is organized as follows: In Section 2, we present a new phytoplankton-fish capture model with a new control strategy that takes into account the density of fish growth as well as the current fish population. In Section 3, we construct the Poincaré map for the model, and then analyze some properties of the Poincaré map. Then, in Section 4, we discuss the existence of

periodic solutions of order- k ($k \geq 1$) of the model, as well as the uniqueness and global stability of periodic solutions of order-1. Then, some numerical simulations are performed in Section 5. Finally, our findings are discussed in Section 6.

2. Model formulation

To formulate our model, we first introduce the following notations:

Table 1. Biological significance of parameters.

parameters	biological significance
$u(t) \in R_+$:	the population of phytoplankton at time $t \in R_+$
$v(t) \in R_+$:	the population of fish at time $t \in R_+$
r :	the intrinsic growth rate of phytoplankton
α :	the absorption rate of phytoplankton by fish
β :	the conversion rate of biomass
d :	the mortality rate of fish
a :	the rate at which phytoplankton release toxins
b :	the half-saturation constant
H :	the threshold at which fish are allowed to be caught
δ :	the maximum capture rate, $0 < \delta < 1$
γ :	the half-saturation constant, $\gamma > 0$
τ :	the reduced number of phytoplankton, $\tau > 0$
θ :	the morphology parameters, $\theta > 0$

Furthermore let $\frac{au}{b+u}$ represent the number of fish, due to the distribution of phytoplankton toxicants, and all parameters are positive and $0 < \delta < 1$. Then, Li et al. proposed the following phytoplankton-fish model with the impulsive feedback control [32]

$$\left\{ \begin{array}{l} \frac{du}{dt} = (r - \alpha v(t))u(t), \\ \frac{dv}{dt} = \left(\beta u(t) - d - \frac{au(t)}{b+u(t)} \right) v(t), \\ u(t^+) = u(t) \left(1 - \frac{\delta u(t)}{u(t)+\gamma} \right) \\ v(t^+) = v(t) - \frac{\tau}{1+\theta v(t)}, \end{array} \right\} \begin{array}{l} v < H, \\ v = H, \end{array} \quad (2.1)$$

Now, it is known that the state pulse capture strategy in (2.1) has certain shortcomings, as it only considers the population size and does not consider the population growth rate. In addition, the control of the pulse model in literature [33, 34] is also single. We propose a feedback control model that considers both population density and population rate, which brings difficulties to the analysis of the model. In literature [32–34], the pulse set and phase set are straight lines on the plane, while in this paper, the phase set is a curve and the determination of phase set is complicated, which also adds a lot of difficulties to the numerical simulation. More precisely, the control threshold is described by

$$a_1 v + b_1 \frac{dv}{dt} = H, \quad (2.2)$$

where a_1 and b_1 are positive constants, satisfying $a_1 + b_1 = 1$, and they are the weight coefficients that control the rate of change in fish population and the rate of change in fish population density, respectively. In real life, we should fish reasonably when $a_1 v + b_1 \frac{dv}{dt} \geq H$ is met. We only assume that fishing is carried out when $a_1 v + b_1 \frac{dv}{dt} = H$ is reached. Then, we reach a model in the following form:

$$\left\{ \begin{array}{l} \frac{du}{dt} = (r - \alpha v(t))u(t), \\ \frac{dv}{dt} = \left(\beta u(t) - d - \frac{au(t)}{b+u(t)} \right) v(t), \\ u(t^+) = u(t) \left(1 - \frac{\delta u(t)}{u(t)+\gamma} \right), \\ v(t^+) = v(t) - \frac{\tau}{1+\theta v(t)}, \end{array} \right\} \begin{array}{l} a_1 v + b_1 \frac{dv}{dt} < H, \\ a_1 v + b_1 \frac{dv}{dt} = H, \end{array} \quad (2.3)$$

which is known as a semi-continuous dynamic system [33, 35]. Without the feedback control, the system (2.3) reduces to an ODE system

$$\left\{ \begin{array}{l} \frac{du}{dt} = (r - \alpha v(t))u(t), \\ \frac{dv}{dt} = \left(\beta u(t) - d - \frac{au(t)}{b+u(t)} \right) v(t). \end{array} \right. \quad (2.4)$$

According to reference [24], we know that system (2.4) has two equilibrium points in the range of real numbers: a saddle point, $O(0,0)$ and a stable positive equilibrium $E^*(u^*, v^*)$, if and only if, $(d + a - \beta b)^2 \geq 4\beta b d$ and $d + a > \beta b$. Where,

$$v^* = \frac{r}{\alpha}, \quad u^* = \frac{d + a - \beta b + \sqrt{(d + a - \beta b)^2 + 4\beta b d}}{2\beta}$$

determined by the intersection of the two nullclines

$$L_1 : v = \frac{r}{\alpha}; \quad L_2 : u = \frac{d + a - \beta b + \sqrt{(d + a - \beta b)^2 + 4\beta b d}}{2\beta}.$$

Next, we construct the Poincaré map to investigate the dynamics of system (2.3).

[Note]: When $\frac{du}{dt} < 0$ and $\frac{dv}{dt} < 0$, the growth rate of its phytoplankton and fish populations is negative. Mathematically speaking, their numbers gradually decrease, and with the increase of time, they will become extinct without control.

3. Poincaré map of system (2.3) and its properties

By using the Eq (2.2) and the second equation in (2.3), we obtain

$$v = \frac{H}{a_1 + b_1 \beta u - b_1 d - \frac{ab_1 u}{b+u}}. \quad (3.1)$$

From a biological point of view, we only consider the properties of the model in region $R_2^+ = \{(u, v), u \geq 0, v \geq 0\}$. To reveal the properties of the Poincaré map, without loss of generality, we assume the initial population size v_0^+ of the fish population satisfies

$$a_1 v_0^+ + b_1 (dv_0^+/dt) < H,$$

and the initial point (u_0^+, v_0^+) satisfies

$$M(v) = \frac{H}{a_1 + b_1\beta\sigma(u) - b_1d - \frac{ab_1\sigma(u)}{b+\sigma(u)}},$$

where $M(v) = \frac{(\theta v - 1) + \sqrt{(\theta v - 1)^2 + 4\theta(\tau + v)}}{2\theta}$. Then, in order to define the impulse set and phase set of the model, we introduce the following sets:

$$\Sigma_N = \left\{ (u, v), u \geq 0, v \geq 0, M(v) = \frac{H}{a_1 + b_1\beta\sigma(u) - b_1d - \frac{ab_1\sigma(u)}{b+\sigma(u)}} \right\},$$

$$\Sigma_M = \left\{ (u, v), u \geq 0, v \geq 0, v = \frac{H}{a_1 + b_1\beta u - b_1d - \frac{ab_1u}{b+u}} \right\},$$

where

$$\sigma(u) = \frac{-\gamma + u + \sqrt{-4\gamma\delta u + \gamma^2 + 2\gamma u + u^2}}{2(1 - \delta)}.$$

We further assume Σ_N and Σ_M intersect with L_2 at A^+ and A^- , respectively, then assume Σ_N and Σ_M intersect with x at $B^1(u^1, 0)$ and $B^2(u^2, 0)$, respectively. Then, depending on the locations of Σ_N and v^* , namely, the positive equilibrium point, we can define the impulse set and phase set of the Poincaré map.

3.1. Case I: $v^* \geq \frac{H}{a_1 + b_1\beta u^* - b_1d - \frac{ab_1u^*}{b+u^*}}$

In this case, E^* is above the impulse set Σ_M (see Figure 1(a)). Thus, there exists a point T on the Σ_N , at which the trajectory of (2.3) is tangent to the Σ_N . Denote the intersection between the trajectory and Σ_M by Q_1 . Then, we define the impulse set by

$$M_1 = \left\{ (u, v) \mid v = \frac{H}{a_1 + b_1\beta u - b_1d - \frac{ab_1u}{b+u}}, u \geq u_{Q_1} \right\},$$

and the phase set by

$$N_1 = \left\{ (u, v) \mid v = \frac{H}{a_1 + b_1\beta\sigma(u) - b_1d - \frac{ab_1\sigma(u)}{b+\sigma(u)}}, u \geq u_{Q_1} \left(1 - \frac{\delta u_{Q_1}}{u_{Q_1} + \gamma} \right) \right\}.$$

3.2. Case II: $v^* < \frac{H}{a_1 + b_1\beta u^* - b_1d - \frac{ab_1u^*}{b+u^*}}$ and $v_{W^-} > \frac{H}{a_1 + b_1\beta\sigma(u^*) - b_1d - \frac{ab_1\sigma(u^*)}{b+\sigma(u^*)}}$

In this case, E^* is below the impulse set Σ_M (see Figure 1(b)). We first assume that Γ_M is the trajectory passing through M in the system. If there is a point W on the Σ_M , so that Γ_W is just tangent to the Σ_M , when $v^* < \frac{H}{a_1 + b_1\beta u^* - b_1d - \frac{ab_1u^*}{b+u^*}}$ and $v_{W^-} > \frac{H}{a_1 + b_1\beta\sigma(u^*) - b_1d - \frac{ab_1\sigma(u^*)}{b+\sigma(u^*)}}$, there must be a point T on the Σ_N so that Γ_T is just tangent to the Σ_N and Γ_T tangent to the Σ_M at the point Q_2 . Then, in this case, we define the impulse set by

$$M_2 = \left\{ (u, v) \mid v = \frac{H}{a_1 + b_1\beta u - b_1d - \frac{ab_1u}{b+u}}, u \geq u_{Q_2} \right\},$$

and the corresponding phase set by

$$N_2 = \left\{ (u, v) \mid v = \frac{H}{a_1 + b_1\beta\sigma(u) - b_1d - \frac{ab_1\sigma(u)}{b+\sigma(u)}}, u \geq u_{Q_2} \left(1 - \frac{\delta u_{Q_2}}{u_{Q_2} + \gamma}\right) \right\}.$$

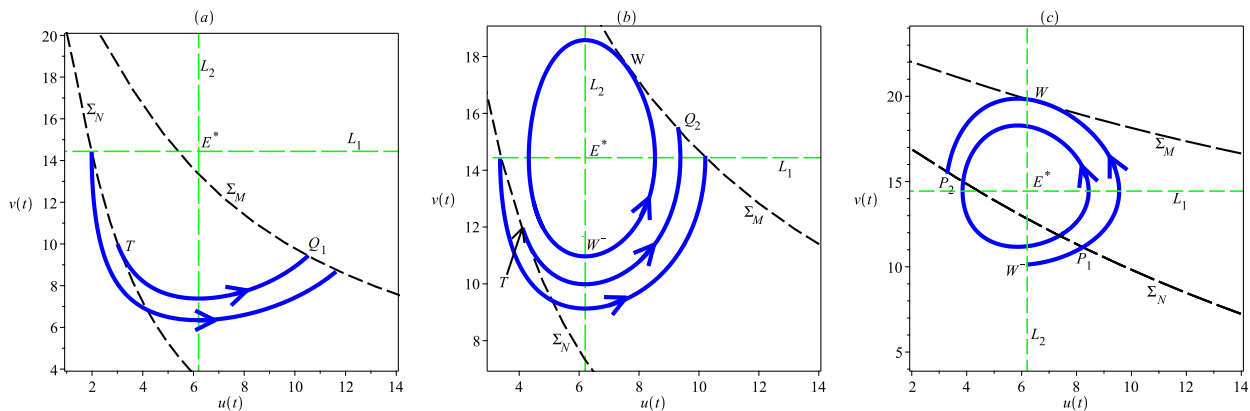


Figure 1. The phase set and impulsive set for Cases I, II and III, respectively.

3.3. Case III: $v_{W^-} < \frac{H}{a_1 + b_1\beta\sigma(u^*) - b_1d - \frac{ab_1\sigma(u^*)}{b+\sigma(u^*)}}$

In this case, E^* is below the impulse set Σ_M , as shown in Figure 1(c). Thus, there is a trajectory denoted by Γ_{W^-} that is tangent to Σ_M at W , and intersects the Σ_N at point P_1 and point P_2 , respectively. Thus, we define the impulse set as

$$M_3 = \left\{ (u, v) \mid v = \frac{H}{a_1 + b_1\beta u - b_1d - \frac{ab_1u}{b+u}}, u \geq u_W \right\},$$

and the phase set as

$$N_3 = \left\{ (u, v) \mid v = \frac{H}{a_1 + b_1\beta\sigma(u^*) - b_1d - \frac{ab_1\sigma(u^*)}{b+\sigma(u^*)}}, u \in (0, u_{P_2}] \cup [u_{P_1}, +\infty) \right\}.$$

Based on the above defined impulse and phase sets, we are now ready to construct the Poincaré map. To this end, let

$$A_k^+ = (u_k^+, v_k^+) = \left(u_k^+, \frac{H}{a_1 + b_1\beta\sigma(u_k^+) - b_1d - \frac{ab_1\sigma(u_k^+)}{b+\sigma(u_k^+)}} \right) \in \Sigma_N,$$

where $0 < u_k^+ < +\infty$, and define the trajectory

$$\pi(t, t_0, A_k^+) \triangleq (u(t, t_0, A_k^+), v(t, t_0, A_k^+))$$

passing through A_k^+ that will reach the Σ_M at point $A_{k+1}(u_{k+1}, v_{k+1})$ at time t_1 , where

$$v_{k+1} = v(t_1, t_0, (u_k^+, v_k^+)) = \frac{H}{a_1 + b_1\beta u_{k+1} - b_1d - \frac{ab_1u_{k+1}}{b+u_{k+1}}}.$$

Then, there is

$$\begin{aligned} u_{k+1}^+ &= u\left(t_1, t_0, \left(u_k^+, \frac{H}{a_1 + b_1\beta\sigma(u_k^+) - b_1d - \frac{ab_1\sigma(u_k^+)}{b+\sigma(u_k^+)}}\right)\right) \\ &\triangleq u\left(u_k^+, \frac{H}{a_1 + b_1\beta\sigma(u_k^+) - b_1d - \frac{ab_1\sigma(u_k^+)}{b+\sigma(u_k^+)}}\right) \triangleq P(u_k^+). \end{aligned}$$

It means that u_{k+1}^+ is determined by u_k^+ . Since point A_{k+1} is on the impulse set, A_{k+1} jump to point

$$A_{k+1}^+ \left(u_{k+1}^+, \frac{H}{a_1 + b_1\beta\sigma(u_{k+1}^+) - b_1d - \frac{ab_1\sigma(u_{k+1}^+)}{b+\sigma(u_{k+1}^+)}} \right),$$

where

$$u_{k+1}^+ = \left(1 - \frac{\delta u_{k+1}}{u_{k+1} + \gamma}\right) u_{k+1} = \left(1 - \frac{\delta P(u_k^+)}{P(u_k^+) + \gamma}\right) P(u_k^+) \triangleq G_m(u_k^+). \quad (3.2)$$

From model (2.3), we obtain

$$\begin{cases} \frac{du}{dv} = \frac{(r - \alpha v)u}{(\beta u - d - \frac{au}{b+u})v} \triangleq w(u, v), \\ u \left(\frac{H}{a_1 + b_1\beta\sigma(u_k^+) - b_1d - \frac{ab_1\sigma(u_k^+)}{b+\sigma(u_k^+)}} \right) = u_0^+. \end{cases} \quad (3.3)$$

Let $v_0^+ = \frac{H}{a_1 + b_1\beta\sigma(u_k^+) - b_1d - \frac{ab_1\sigma(u_k^+)}{b+\sigma(u_k^+)}}$, $u_0^+ = S$, then we obtain that (u_0^+, v_0^+) is in Σ_N .

We define

$$u(v) = u\left(S, \frac{H}{a_1 + b_1\beta\sigma(u_k^+) - b_1d - \frac{ab_1\sigma(u_k^+)}{b+\sigma(u_k^+)}}\right) \triangleq u(S, v).$$

Then, according to the model (3.2),

$$u(S, v) = S + \int_{\frac{H}{a_1 + b_1\beta\sigma(u_k^+) - b_1d - \frac{ab_1\sigma(u_k^+)}{b+\sigma(u_k^+)}}}^v \omega(u(S, s), s) ds. \quad (3.4)$$

From Eqs (3.2) and (3.3), the Poincaré map expression of system (2.2) is

$$G_m(S) = \left(1 - \frac{\delta u \left(S, \frac{H}{a_1 + b_1 \beta \sigma(u_k^+) - b_1 d - \frac{ab_1 \sigma(u_k^+)}{b + \sigma(u_k^+)}} \right)}{u \left(S, \frac{H}{a_1 + b_1 \beta \sigma(u_k^+) - b_1 d - \frac{ab_1 \sigma(u_k^+)}{b + \sigma(u_k^+)}} \right) + \gamma} \right) u \left(S, \frac{H}{a_1 + b_1 \beta \sigma(u_k^+) - b_1 d - \frac{ab_1 \sigma(u_k^+)}{b + \sigma(u_k^+)}} \right). \quad (3.5)$$

Then, we can show that it has the following properties in Theorem 3.1.

Theorem 3.1. If $\frac{H}{a_1 + b_1 \beta u^* - b_1 d - \frac{ab_1 u^*}{b + u^*}} < v^*$, then the trajectory Γ_T intersects with Σ_M at point $Q_1(u_{Q_1}, v_{Q_1})$, and we have:

- (i) The domain of $G_m(S)$ is $(0, u^1)$, $G_m(S)$ is monotonically decreasing on $(0, u_T]$, and monotonically increasing on (u_T, u^1) .
- (ii) $G_m(S)$ is continuously differentiable on $(0, u^1)$.
- (iii) When $G_m(u_T) > u_T$, it has a unique fixed point on $(u_T, +\infty)$ (see Figure 2(b)). When $G_m(u_T) < u_T$, it has a unique fixed point on $(0, u_T)$ (see Figure 2(a)). When $G_m(u_T) = u_T$, u_T is the fixed point.

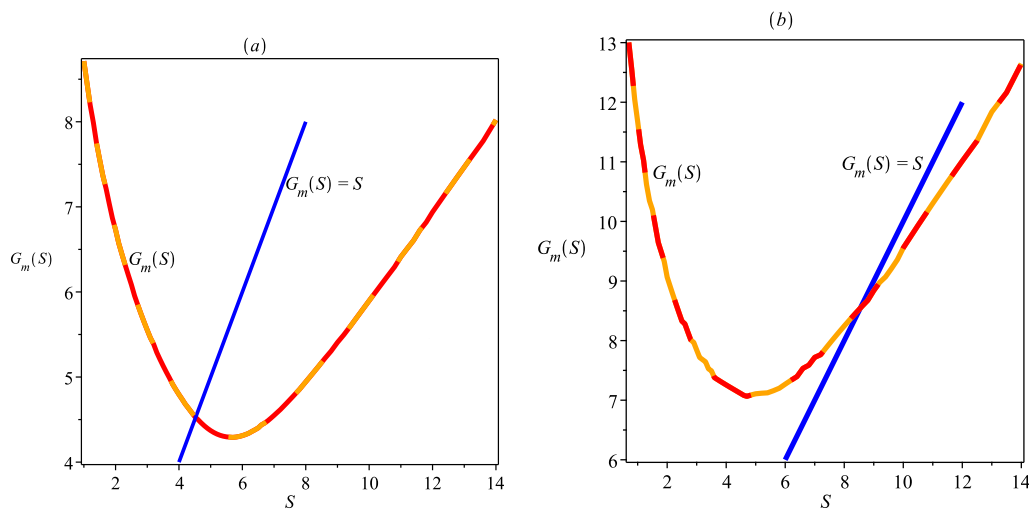


Figure 2. The Poincaré map $G_m(S)$ related to the impulsive point series S . The parameter values are as follows: $r = 1.444$, $\alpha = 0.1$, $\beta = 0.1$, $d = 0.5$, $a = 0.1$, $b = 1$, $\delta = 0.4$, $\gamma = 1$. (c) $a_1 = 0.8$, $b_1 = 0.2$, $H = 16$, $\theta = 0.6$, $\tau = 16$. (b) $H = 15$, $\theta = 1$, $\tau = 18$.

Proof. (i) Note that $E^*(u^*, v^*)$ is a linear center and $\frac{H}{a_1 + b_1 \beta u^* - b_1 d - \frac{ab_1 u^*}{b + u^*}} < v^*$. Taking any point $A_k^+(u_k^+, v_k^+)$ on Σ_N , the trajectory $\Gamma_{A_k^+}$ will reach the M_1 . So the domain of $G_m(S)$ is $(0, u^1)$.

For any $u_{k_1}^+, u_{k_2}^+ \in [u_T, u^1)$, and where $u_{k_1}^+ < u_{k_2}^+$, it is easy to get

$$\mu(u_{k_1}^+, v_{k_1}^+) < \mu(u_{k_2}^+, v_{k_1}^+),$$

which implies that there is $G_m(u_{k_1}^+) < G_m(u_{k_2}^+)$. Therefore, $G_m(S)$ is monotonically increasing on $[u_T, u^1]$.

When $u_{k_1}^+, u_{k_2}^+ \in (0, u_T)$, $u_{k_1}^+ < u_{k_2}^+$. The trajectory $\Gamma_{A_{k_1}^+}$ from point $A_{k_1}^+(u_{k_1}^+, v_{k_1}^+)$ and the trajectory $\Gamma_{A_{k_2}^+}$ from point $A_{k_2}^+(u_{k_2}^+, v_{k_2}^+)$ will pass through L_2 and intersect Σ_N at points $A_{k_{11}}^+(u_{k_{11}}^+, v_{k_{11}}^+)$ and $A_{k_{21}}^+(u_{k_{21}}^+, v_{k_{21}}^+)$, respectively. Here $u_{k_{i1}}^+ (i = 1, 2) \in [u_T, u^1]$ and $u_{k_{11}}^+ > u_{k_{21}}^+$. It can be seen that $G_m(u_{k_1}^+) > G_m(u_{k_2}^+)$. Therefore, $G_m(S)$ is monotonically decreasing on $(0, u_T)$.

(ii) Equation (3.2) suggests that $w(u, v)$ is continuously differentiable. Thus, $G_m(S)$ is continuously differentiable in the first quadrant.

(iii) When $G_m(u_T) = u_T$, then u_T is the fixed point of function $G_m(S)$.

If $G_m(u_T) > u_T$, $G_m(u_T) - u_T > 0$. Since $0 < \delta < 1$, there must be a value S^* , such that

$$G_m(S^*) = S^* \left(1 - \frac{\delta S^*}{S^* + \gamma} \right) = S^* \left(1 - \delta - \frac{\delta \gamma}{S^* + \gamma} \right) < S^* (1 - \delta) < S^*.$$

So there is at least one $\tilde{u} \in (u_T, S^*)$, satisfying $G_m(\tilde{u}) = \tilde{u}$.

When $G_m(u_T) < u_T$, let $G_m(u_T) = u_1 < u_T$. We know that $G_m(S)$ is monotonically decreasing on $(0, u_T]$, so $G_m(u_1) > G_m(u_T) = u_1$, and because $G_m(u_T) < u_T$, so there is at least one $\tilde{u} \in (u_1, u_T)$, satisfies $G_m(\tilde{u}) = \tilde{u}$.

From the above analysis, we know that $G_m(S)$ has at least one fixed point. Next, we prove the uniqueness by contradiction. Assume the system has two fixed points, \tilde{u}_1 and \tilde{u}_2 respectively, so that $G_m(\tilde{u}_1) = \tilde{u}_1$ and $G_m(\tilde{u}_2) = \tilde{u}_2$. Let $\tilde{u}_1 < \tilde{u}_2$, we define

$$d_{\tilde{u}_1 \tilde{u}_2}(u) = u(v, \tilde{u}_2) - u(v, \tilde{u}_1).$$

Differentiate the last equation with respect to t obtain

$$\begin{aligned} d'_{\tilde{u}_1 \tilde{u}_2}(u) &= u'(v, \tilde{u}_2) - u'(v, \tilde{u}_1) \\ &= \frac{r-\alpha v}{v} \left[\frac{\tilde{u}_2}{\beta \tilde{u}_2 - d - \frac{a\tilde{u}_2}{b+\tilde{u}_2}} - \frac{\tilde{u}_1}{\beta \tilde{u}_1 - d - \frac{a\tilde{u}_1}{b+\tilde{u}_1}} \right]. \end{aligned}$$

Let

$$g(u) = \frac{u}{\beta u - d - \frac{au}{b+u}},$$

then

$$g'(u) = \frac{-d - a\left(\frac{u}{b+u}\right)^2}{\left(\beta u - d - \frac{au}{b+u}\right)^2} < 0,$$

so

$$g(\tilde{u}_2) < g(\tilde{u}_1),$$

that is

$$d'_{\tilde{u}_1 \tilde{u}_2}(u) < 0,$$

i.e.

$$d_{\tilde{u}_1\tilde{u}_2}(a_1 + b_1\beta\sigma(u_k^+) - b_1d - \frac{ab_1\sigma(u_k^+)}{b + \sigma(u_k^+)}) > d_{\tilde{u}_1\tilde{u}_2}(a_1 + b_1\beta u_k^+ - b_1d - \frac{ab_1u_k^+}{b + u_k^+}).$$

From system (2.3):

$$\begin{aligned} \tilde{u}_1 &= \mu(\tilde{u}_1) \left(1 - \frac{\delta\mu(\tilde{u}_1)}{\mu(\tilde{u}_1)+\gamma}\right) \\ &= \mu(\tilde{u}_1) \left(1 - \delta + \frac{\delta\gamma}{\mu(\tilde{u}_1)+\gamma}\right) \\ &= \left[\mu(\tilde{u}_2) - d_{\tilde{u}_1\tilde{u}_2}(a_1 + b_1\beta u_k^+ - b_1d - \frac{ab_1u_k^+}{b+u_k^+})\right] \left(1 - \delta + \frac{\delta\gamma}{\mu(\tilde{u}_1)+\gamma}\right) \\ &= \mu(\tilde{u}_2) \left(1 - \delta + \frac{\delta\gamma}{\mu(\tilde{u}_1)+\gamma}\right) - d_{\tilde{u}_1\tilde{u}_2}(a_1 + b_1\beta u_k^+ - b_1d - \frac{ab_1u_k^+}{b+u_k^+}) \left(1 - \delta + \frac{\delta\gamma}{\mu(\tilde{u}_1)+\gamma}\right) \\ &> \mu(\tilde{u}_2) \left(1 - \delta + \frac{\delta\gamma}{\mu(\tilde{u}_2)+\gamma}\right) - \frac{\tilde{u}_1 d_{\tilde{u}_1\tilde{u}_2}(a_1 + b_1\beta u_k^+ - b_1d - \frac{ab_1u_k^+}{b+u_k^+})}{\mu(\tilde{u}_1)} \\ &= \tilde{u}_2 - \frac{\tilde{u}_1 d_{\tilde{u}_1\tilde{u}_2}(a_1 + b_1\beta u_k^+ - b_1d - \frac{ab_1u_k^+}{b+u_k^+})}{\mu(\tilde{u}_1)}, \end{aligned}$$

that is

$$\frac{\tilde{u}_1 d_{\tilde{u}_1\tilde{u}_2}(a_1 + b_1\beta u_k^+ - b_1d - \frac{ab_1u_k^+}{b+u_k^+})}{\mu(\tilde{u}_1)} > \tilde{u}_2 - \tilde{u}_1 = d_{\tilde{u}_1\tilde{u}_2} \left(a_1 + b_1\beta\sigma(u_k^+) - b_1d - \frac{ab_1\sigma(u_k^+)}{b + \sigma(u_k^+)}\right).$$

It is easy to know that $\frac{\tilde{u}_1}{\mu(\tilde{u}_1)} < 1$ if $a_1 + b_1\beta u^* - b_1d - \frac{ab_1u^*}{b+u^*} < v^*$, so

$$\begin{aligned} &d_{\tilde{u}_1\tilde{u}_2}(a_1 + b_1\beta u_k^+ - b_1d - \frac{ab_1u_k^+}{b+u_k^+}) \\ &> \frac{\tilde{u}_1 d_{\tilde{u}_1\tilde{u}_2}(a_1 + b_1\beta u_k^+ - b_1d - \frac{ab_1u_k^+}{b+u_k^+})}{\mu(\tilde{u}_1)} \\ &> d_{\tilde{u}_1\tilde{u}_2} \left(a_1 + b_1\beta\sigma(u_k^+) - b_1d - \frac{ab_1\sigma(u_k^+)}{b + \sigma(u_k^+)}\right), \end{aligned}$$

which is contradictory with

$$d_{\tilde{u}_1\tilde{u}_2} \left(a_1 + b_1\beta\sigma(u_k^+) - b_1d - \frac{ab_1\sigma(u_k^+)}{b + \sigma(u_k^+)}\right) > d_{\tilde{u}_1\tilde{u}_2} \left(a_1 + b_1\beta u_k^+ - b_1d - \frac{ab_1u_k^+}{b + u_k^+}\right).$$

The fixed point is unique. □

When $\frac{H}{a_1 + b_1\beta u^* - b_1d - \frac{ab_1u^*}{b+u^*}} > v^*$ and Γ_T intersects with Σ_M (case II), $G_m(S)$ of system (2.3) has similar properties with case I.

Theorem 3.2. Suppose $\frac{H}{a_1 + b_1\beta u^* - b_1d - \frac{ab_1u^*}{b+u^*}} > v^*$. Then, then trajectory Γ_{W^-} is tangent to Σ_M at W and intersect Σ_N at point $P_1(u_{P_1}, v_{P_1})$ and point $P_2(u_{P_2}, v_{P_2})$, respectively, where $u_{P_1} > u_{P_2}$. Furthermore, $G_m(S)$ has the following properties:

- (i) The domain of $G_m(S)$ is $(0, u_{P_2}] \cup [u_{P_1}, u^1)$, and $G_m(S)$ is monotonically decreasing on $(0, u_{P_2}]$ and monotonically increasing on $[u_{P_1}, u^1)$.

(ii) When $G_m(u_{P_2}) \leq u_{P_2}$, there is a unique fixed point on $(0, u_{P_2}]$ (see Figure 3(a)). When $G_m(u_{P_2}) > u_{P_2}$, there is no fixed point (see Figure 3(b)).

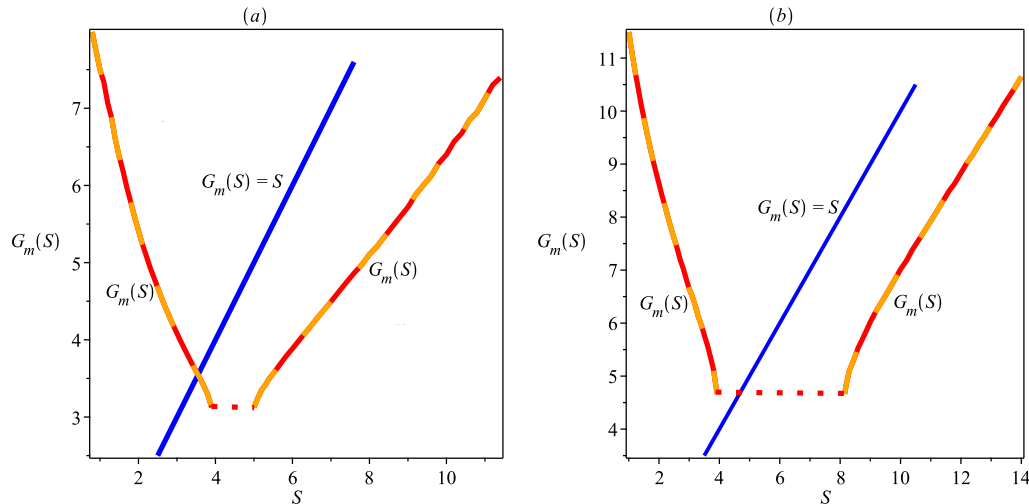


Figure 3. The Poincaré map $G_m(S)$ related to the impulsive point series S . The parameter values are as follows: $r = 1.444$, $\alpha = 0.1$, $\beta = 0.15$, $d = 0.5$, $a = 0.5$, $b = 1$, $\gamma = 1$. (a) $a_1 = 0.6$, $b_1 = 0.4$, $H = 13$, $\delta = 0.7$, $\theta = 1$, $\tau = 18$. (b) $a_1 = 0.8$, $b_1 = 0.2$, $H = 16$, $\delta = 0.4$, $\theta = 0.6$, $\tau = 65$.

Proof. (i) Because $E^*(u^*, v^*)$ is the center point, if $\frac{H}{a_1 + b_1 \beta u^* - b_1 d - \frac{ab_1 u^*}{b + u^*}} > v^*$ and the trajectory Γ_{W^-} is tangent to Σ_M at W and intersect with the Σ_N at point $P_1(u_{P_1}, v_{P_1})$ and point $P_2(u_{P_2}, v_{P_2})$, respectively, $u_{P_1} > u_{P_2}$. Then, take any point $A_k^+(u_k^+, v_k^+)$ in Σ_N , if $u_k^+ \in (0, u_{P_2}] \cup [u_{P_1}, +\infty)$, the trajectory $\Gamma_{A_k^+}$ will reach the M_3 at point $A_{k+1}(u_k, v_k)$, if $u_k^+ \in (u_{P_2}, u_{P_1})$ the $\Gamma_{A_k^+}$ has no intersection with the M_3 . So the domain of $G_m(S)$ is $(0, u_{P_2}] \cup [u_{P_1}, u^1)$.

For any $u_{k_1}^+, u_{k_2}^+ \in [u_{P_1}, u^1)$ and $u_{k_1}^+ < u_{k_2}^+$ easy to get

$$\mu(u_{k_1}^+, v_{k_1}^+) < \mu(u_{k_2}^+, v_{k_2}^+),$$

so $G_m(u_{k_1}^+) < G_m(u_{k_2}^+)$. Therefore, $G_m(S)$ is monotonically increasing on $[u_{P_1}, u^1)$.

When $u_{k_1}^+, u_{k_2}^+ \in (0, u_{P_2}]$, $u_{k_1}^+ < u_{k_2}^+$. The trajectory from $A_{k_1}^+(u_{k_1}^+, v_{k_1}^+)$ and $A_{k_2}^+(u_{k_2}^+, v_{k_2}^+)$ will pass through the L_2 intersect with the Σ_N at point $A_{k_{11}}^+(u_{k_{11}}^+, v_{k_{11}}^+)$ and point $A_{k_{21}}^+(u_{k_{21}}^+, v_{k_{21}}^+)$, respectively. Then, $u_{k_{11}}^+ (i = 1, 2) \in [u_{32}, u^1)$ and $u_{k_{11}}^+ > u_{k_{21}}^+$. So $G_m(u_{k_1}^+) > G_m(u_{k_2}^+)$, therefore, $G_m(S)$ is monotonically decreasing on $(0, u_{P_2}]$.

(ii) Consider the relationship between $G_m(u_{P_2})$ and u_{P_2} :

(a) When $G_m(u_{P_2}) \leq u_{P_2}$ (see Figure 3(a)), we assume $G_m(u_{P_2}) = u_1 \leq u_{P_2}$. We know that $G_m(S)$ is monotonically decreasing on $(0, u_{P_2}]$, so $G_m(u_{P_2}) \geq G_m(u_{P_2}) = u_1$, and because $G_m(u_{P_2}) \leq u_{P_2}$, so there is a point $\tilde{u} \in (u_1, u_{P_2}]$ satisfies $G_m(\tilde{u}) = \tilde{u}$.

(b) When $G_m(u_{P_2}) > u_{P_2}$ (see Figure 3(b)), there is no $\tilde{u} \in (0, u_{P_2}]$ to satisfies $G_m(\tilde{u}) = \tilde{u}$.

For any $u_k \in (u_{P_1}, u^1)$, trajectory of point $A_k(u_k, v_k)$ on Σ_N is tangent to the Σ_M at point $A_k^+(u_k^+, v_k^+)$. The point $A_k^+(u_k^+, v_k^+)$ will be pulsed to $A_{k+1}(u_{k+1}, v_{k+1})$. To get $u_{k+1} < u_k^+ < u_k$, that is $u_{k+1} \neq u_k$, so there is no $\tilde{u} \in (u_{P_1}, u^1)$ satisfies $G_m(\tilde{u}) = \tilde{u}$. \square

4. The order- k ($k \geq 1$) periodic solution of the semi-continuous dynamic system (2.3) and its stability

Theorem 3.1 has proved that system (2.3) has a fixed point under certain conditions, that is, the system has an order-1 periodic solution. Below, we will give more properties of the order-1 solution, and also the existence of the order- k solutions.

Theorem 4.1. *The order-1 periodic solution of system (2.3) is globally asymptotically stable if $\frac{H}{a_1 + b_1 \beta u^* - b_1 d - \frac{ab_1 u^*}{b + u^*}} < v^*$ and $G_m(u_{Q_1}) > u_{Q_1}$.*

Proof. When $G_m(u_{Q_1}) > u_{Q_1}$, $G_m(S)$ has a fixed point \tilde{u} on (u_{Q_1}, u^1) , that is, $G_m(\tilde{u}) = \tilde{u}$ from the (iii) of Theorem 3.1. For any point $A_0^+(u_0^+, v_0^+)$ in Σ_N , where $u_0^+ > u_{Q_1}$, $\Gamma_{A_0^+}$ will intersect Σ_M at the point $p_1^+(u_1^+, v_1^+)$, which is $G_m(u_0^+) = u_1^+$, repeating the above process,

$$G_m(G_m(u_0^+)) = G_m^2(u_0^+),$$

that is,

$$G_m(u_1^+) = u_2^+,$$

further available,

$$u_n^+ = G_m^n(u_0^+), n = 1, 2, \dots$$

Then, we have the following three cases:

Case 1: $u_{Q_1} < u_0^+ \leq \tilde{u}$. Since $G_m(u_{Q_1}) > u_{Q_1}$ and $G_m(S)$ is monotonously increasing on $(u_{Q_1}, +\infty)$. Let $G_m(u_i^+) = u_{i+1}^+$ yields

$$\begin{aligned} u_0^+ &< G_m(u_0^+) = u_1^+ \leq G_m(\tilde{u}) = \tilde{u}, \\ u_0^+ &< G_m(u_0^+) < G_m(u_1^+) = G_m^2(u_0^+) \leq G_m(\tilde{u}) = \tilde{u}, \end{aligned}$$

Following the same fashion, we obtain that

$$u_0^+ < G_m(u_0^+) < \dots < G_m^n(u_0^+) < \dots < \tilde{u}.$$

Then we can get

$$\lim_{n \rightarrow +\infty} G_m^n(u_0^+) = \tilde{u}.$$

Case 2: $\tilde{u} < u_0^+ < u^1$. In this case, we have

$$\tilde{u} = G_m(\tilde{u}) < G_m(u_0^+),$$

and

$$\tilde{u} = G_m(\tilde{u}) < G_m^2(u_0^+) < G(u_0^+).$$

By mathematical induction,

$$\tilde{u} = G_m(\tilde{u}) < \dots < G_m^n(u_0^+) < G_m^{n-1}(u_0^+) < \dots$$

Thus,

$$\lim_{n \rightarrow +\infty} G_m^n(u_0^+) = \tilde{u}.$$

Case 3: $0 < u_0^+ < u_{Q_1}$. Since $G_m(u_{Q_1}) > u_{Q_1}$ and $G_m(S)$ is decreasing on $(0, u_{Q_1})$, we obtain that $G_m(u_0^+) > G_m(u_{Q_1}) > u_{Q_1}$ for any $u_0^+ \in (0, u_{Q_1})$. So, we can conclude that $G_m(u_0^+) > u_{Q_1}$. When $u_{Q_1} < G_m(u_0^+) < \tilde{u}$, this is the situation in Case 1; when $G_m(u_0^+) > \tilde{u}$, this is Case 2 above.

Thus, we always have

$$\lim_{n \rightarrow +\infty} G_m^n(u_0^+) = \tilde{u}.$$

The conclusion is proved. \square

Theorem 4.2. *The semi-continuous dynamical system (2.3) has a stable order-1 periodic solution or an order-2 periodic solution when $\frac{H}{a_1 + b_1 \beta u^* - b_1 d - \frac{ab_1 u^*}{b + u^*}} < v^*$, $G_m(u_{Q_1}) < u_{Q_1}$ and $G_m^2(u_{Q_1}) < u_{Q_1}$.*

Proof. Take a point $A_0^+(u_0^+, v_0^+)$ on Σ_N . Since E^* is a center point, $\Gamma_{A_0^+}$ will intersect Σ_M at point $A_1(u_1, v_1)$, where $u_1 = \mu(u_0^+, v_0^+)$. p_1 will reach point $p_1^+(u_1^+, v_1^+)$ by an impulse, so $G_m(u_0^+) = u_1^+$. Repeat the above process

$$u_n^+ = G_m^n(u_0^+) = G_m(G_m^{n-1}(u_0^+)), \quad (n = 1, 2, \dots).$$

When $u_{Q_1} \leq u_0^+ < u^1$, $G_m(S)$ is increasing on $[u_{Q_1}, u^1)$ and from the (i) of Theorem 3.1, we know there is no fixed point on $[u_{Q_1}, u^1)$. Therefore, there is a positive integer i that satisfies

$$u_{i-1}^+ = G_m(u_{i-2}^+) < u_{Q_1}$$

and

$$u_i^+ = G_m(u_{i-1}^+) < G_m(u_{Q_1}) < u_{Q_1}.$$

When $0 < u_0^+ < u_{Q_1}$, the $\Gamma_{A_0^+}$ will pass through the L_2 and intersects the Σ_N at $p'_0(u'_0, H - \frac{\tau}{1+\theta H})$, where $0 < u'_0 < u_{Q_1}$, this can be transformed into the above situation.

So, for any $u_0^+ \in (0, u^1)$, there always be i satisfies

$$G_m(u_{Q_1}) < G_m^i(u_0^+) < u_{Q_1} \quad (i \geq 1).$$

So, we just consider the initial point $p_0^+(u_0^+, v_0^+)$, where $u_{Q_1} \leq u_0^+ < G_m(u_{Q_1})$. Since $G_m(S)$ is monotonically decreasing on $[G_m(u_{Q_1}), u_{Q_1}]$, we have

$$G_m[G_m(u_{Q_1}), u_{Q_1}] \subset [G_m(u_{Q_1}), u_{Q_1}].$$

Let $G_m(u_0^+) \neq u_0^+$ and $G_m^2(u_0^+) \neq u_0^+$. Consider the following four situations:

Case I: $u_{Q_1} \geq u_0^+ > G_m^2(u_0^+) > G_m(u_0^+) \geq G_m(u_{Q_1})$. According to the monotonicity of $G_m(S)$:

$$u_2^+ = G_m(u_1^+) > G_m(u_2^+) = u_3^+ > G_m(u_0^+) = u_1^+,$$

furthermore,

$$u_4^+ = G_m(u_3^+) < G_m(u_0^+) = u_0^+.$$

Thus, there is

$$u_{Q_1} \geq u_0^+ > u_2^+ > u_4^+ > u_3^+ > u_1^+ \geq G_m(u_{Q_1}).$$

Proved by mathematical induction:

$$u_{Q_1} \geq u_0^+ > u_2^+ > \dots > u_{2n}^+ > u_{2n+2}^+ > \dots > u_{2n+1}^+ > u_{2n-1}^+ > \dots > u_1^+ \geq G_m(u_{Q_1}).$$

Case II: $u_{Q_1} \geq u_1^+ > u_0^+ > u_2^+ \geq G_m(u_{Q_1})$. $G_m(S)$ is monotonically decreasing on $[G_m(u_{Q_1}), u_{Q_1}]$. So,

$$u_3^+ = G_m(u_2^+) > G_m(u_0^+) = u_1^+ > G_m(u_1^+) = u_2^+,$$

and

$$u_4^+ = G_m(u_3^+) < G_m(u_1^+) = u_2^+ < G_m(u_2^+) = u_3^+,$$

then

$$u_{Q_1} \geq u_3^+ > u_1^+ > u_0^+ > u_2^+ > u_4^+ \geq G(u_{Q_1}),$$

so

$$u_{Q_1} \geq \dots > u_{2n+1}^+ > u_{2n-1}^+ > \dots > u_3^+ > u_1^+ > u_0^+ > u_2^+ > u_4^+ > \dots > u_{2n}^+ > \dots \geq G(u_{Q_1}).$$

Case III: $u_{Q_1} \geq u_1^+ > u_2^+ > u_0^+ \geq G_m(u_{Q_1})$.

To get

$$u_{Q_1} \geq u_1^+ > u_3^+ > \dots > u_{2n-1}^+ > \dots > u_{2n+1}^+ > u_{2n}^+ > \dots > u_2^+ > u_0^+ \geq G_m(u_{Q_1}).$$

Case IV: $u_{Q_1} \geq u_2^+ > u_0^+ > u_1^+ \geq G_m(u_{Q_1})$.

This situation is similar to Case I, can get

$$G_m(u_{Q_1}) \leq u_{2n+1}^+ < u_{2n-1}^+ < \dots < u_1^+ < u_0^+ < u_2^+ < \dots < u_{2n}^+ < u_{2n+1}^+ < \dots \leq u_{Q_1}.$$

For Case I and Case III, there is $\tilde{u} \in (u_{Q_1}, G_m(u_{Q_1}))$, so that

$$\lim_{n \rightarrow \infty} u_{2n}^+ = \lim_{n \rightarrow \infty} u_{2n-1}^+ = \tilde{u},$$

That is to say, in these two cases, system (2.3) has a stable order-1 periodic solution.

For case II and case IV, $\tilde{u}_1 \neq \tilde{u}_2$ and

$$\begin{aligned} \lim_{n \rightarrow \infty} u_{2n-1}^+ &= \tilde{u}_1, \\ \lim_{n \rightarrow \infty} u_{2n}^+ &= \tilde{u}_2, \end{aligned}$$

That is to say, system (2.3) has a stable order-2 periodic solution in these two cases. \square

Theorem 4.3. Let $H_1 < u_{Q_1}$ and $G_m(u_{Q_1}) < u_{Q_1}$. Then, the necessary and sufficient condition for the order-1 periodic solution of system (2.3) to be globally stable is $G_m^2(u^+) < u^+$ for any $u^+ \in (0, u_{Q_1}]$.

Proof. Sufficiency:

When $G_m(u_{Q_1}) < u_{Q_1}$, there exists $\tilde{u} \in (G_m(u_{Q_1}), u_{Q_1})$ which satisfies $G_m(\tilde{u}) = \tilde{u}$.

For any $u^+ \in (\tilde{u}, u_{Q_1})$, we make $u_1^+ = G_m(u^+)$ and $u_2^+ = G_m(u_1^+) = G_m^2(u^+)$, since $G_m^2(u^+) < u^+ < u_{Q_1}$ to get $\tilde{u} > u_1^+ > G_m(u_{Q_1}), u_{Q_1} > u_2^+ > u_4^+ > \tilde{u} > u_3^+ > u_1^+ > G_m(u_{Q_1})$, so, $u_{Q_1} > u_{2n}^+ > \tilde{u} > u_{2n+1}^+ > G_m(u_{Q_1})$.
So

$$\lim_{n \rightarrow \infty} u_{2n}^+ = \lim_{n \rightarrow \infty} u_{2n+1}^+ = \tilde{u}.$$

Necessity: If $G_m^2(u^+) < u^+$ is not true for any $u^+ \in [\tilde{u}, u_{Q_1}]$, there exists a maximum $u_0 \in [\tilde{u}, u_{Q_1}]$ satisfies $G_m^2(u_0) \geq u_0$. There u_1 and $G_m^2(u_1) < u_1$ for any $\tilde{u} - \varepsilon < u_1 < \tilde{u} + \varepsilon$, where $\varepsilon > 0$. From the continuity of $G_m^2(u)$ on the $[u_0, u_1]$ there is at least one $\vec{u} \in [u_0, u_1]$ and $G_m^2(\vec{u}) = \vec{u}$. This is contradictory. \square

Theorem 4.4. If $G_m(u_{Q_1}) < u_{Q_1}$ and there is u_m^+ , such that $u_m^+ = \min\{u^+ : G_m(u^+) = u_{Q_1}\}$, the system (2.3) has a order-3 periodic solution if $G_m^2(u_{Q_1}) < u_m^+$.

Proof. If $G_m(u_{Q_1}) < u_{Q_1}$, there is a order-1 periodic solution in $(G_m(u_{Q_1}), u_{Q_1})$, i.e., $G_m(\tilde{u}) = \tilde{u}$, here, $\tilde{u} \in (G_m(u_{Q_1}), u_{Q_1})$. Since $G_m(\tilde{u}) = \tilde{u}$, so there is u_m^+ such that $u_m^+ \in (0, \tilde{u})$ and $G_m(u_m^+) = u_{Q_1}$. Further, $G_m^3(u_m^+) = G_m^2(u_{Q_1}) < u_m^+$, on the other hand, $\lim_{x \rightarrow 0} G_m^3(x) > x$, so there is at least one value of \vec{u} , such that $G_m^3(\vec{u}) = \vec{u}$. \square

Remark 4.1. Using the similar arguments, we can show that if $G_m^{k-1}(u_{Q_1}) < u_m^+$, where $G_m(u_m^+) = u_{Q_1}$, then the system (2.3) has an order- k ($k \geq 2$) periodic solution.

[Note]: Global asymptotic stability means: A solution $u(t)$ is called asymptotically stable if it is stable and there exists a number $\varepsilon_0 > 0$, such that, for any other solution $v(t)$ with $\|u(t_0) - v(t_0)\| < \varepsilon_0$, the following holds: $\lim_{t \rightarrow \infty} \|u(t) - v(t)\| = 0$ [35].

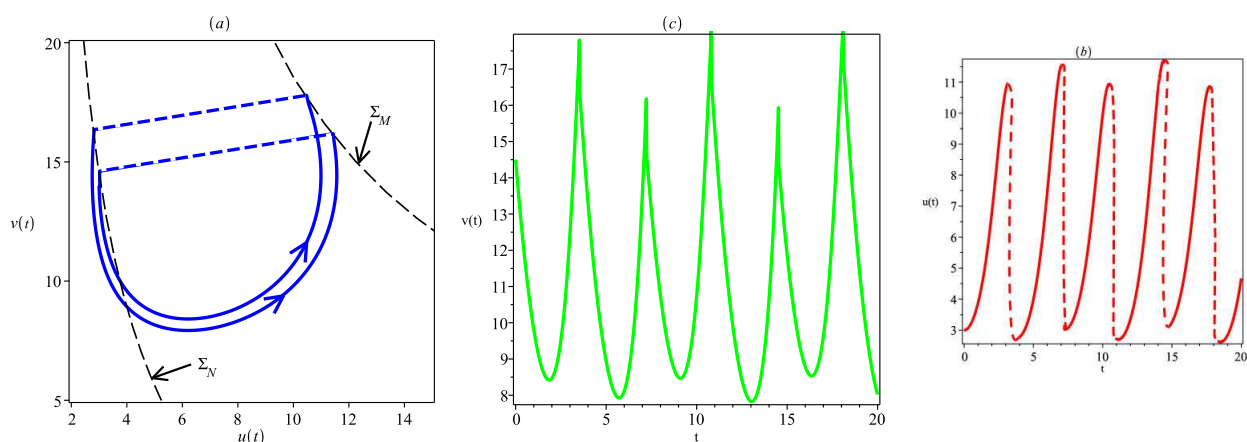


Figure 4. The order-2 periodic solution of Cases III.

5. Simulations and discussion

In this section, we carry out some numerical simulations, illustrating our theoretical findings in previous sections and then discuss these results from a biological point of view.

Figure 4(a) is the trajectory of the order-2 periodic solution of the model. Figure 4(b),(c) is the time series of phytoplankton density and fish density under the simulated order-2 periodic solution, respectively. The existence of the order-2 periodic solution of the system indicates that after two fishing in a period of time, the population returns to the initial point, so the population shows this stable periodic change.

In Figure 5(a), we numerically illustrate our mathematical findings in Theorem 3.2, corresponding to the cases in Figure 3. In sub-figure a, we see the only order-1 periodic solution (see Figure 5(a)), and in the case of Figure 3(b), there is no order-1 periodic solution (see Figure 5(b)).

Figure 6 shows that when the weight parameters a_1 and b_1 change, the pulse and phase sets change significantly. That is to say, the comprehensive fishing measures that comprehensively consider the fish population density and the current fish growth rate are compared to the fishing measures that only consider the fish population density. The model will generate more complex pulse sets and phase sets. Below, we discuss which of the two fishing measures is more biologically appropriate.

From Figure 7, we see that, no matter what the value of r is, the smaller the weight of a_1 , the greater the weight of b_1 , the longer the single period of the order-1 periodic solution, that is, the comprehensive control measures that take into account the fish population density and the current growth rate are longer than the cycle time of the system that only considers the fish population density. That is, the comprehensive fishing measures that comprehensively consider the fish population density and the current fish growth rate are more reasonable than the fishing measures that only consider the fish population density.

It can be seen from Figure 8 that the trajectories of different initial points, eventually. This illustrates the global asymptotic stability of the order-1 periodic solution. This provides theoretical support for the application of state-dependent feedback control in ecosystem balance.

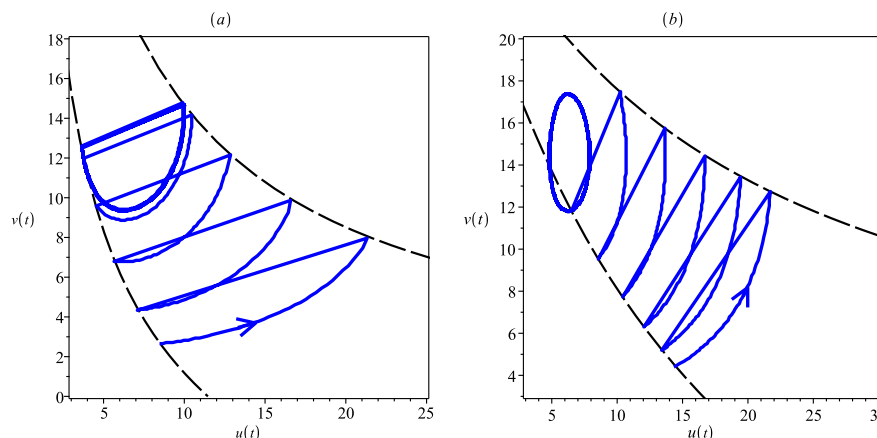


Figure 5. Periodic solutions in the case of Figures 3 (a) and (b), respectively.

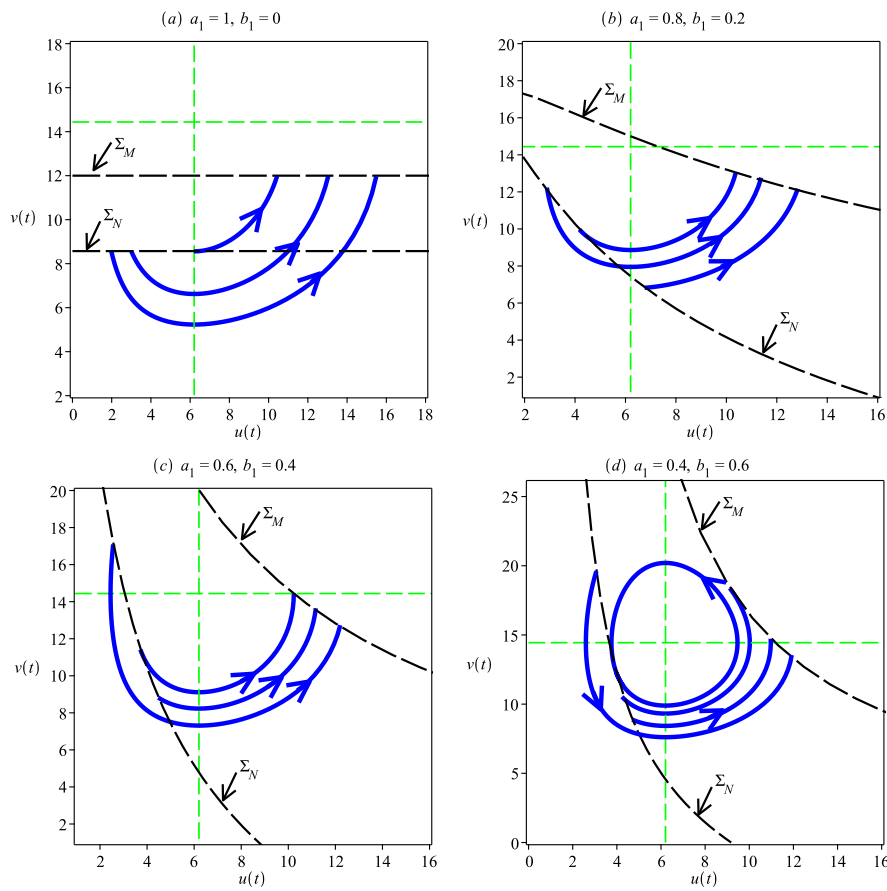


Figure 6. The impulse and phase sets of the system (2.3) with different weighted parameters a_1 and b_1 .

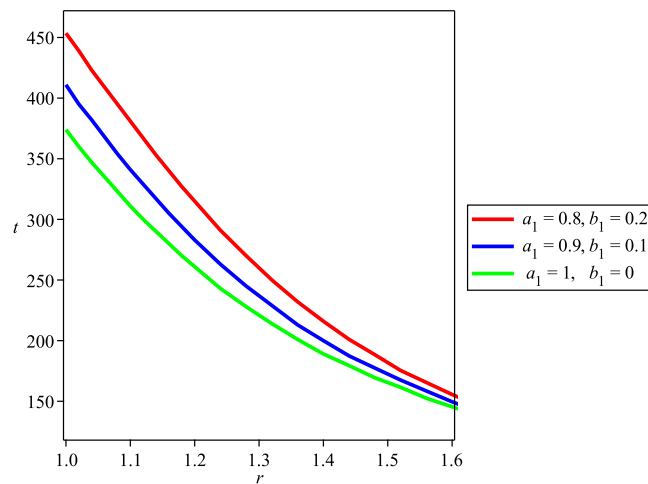


Figure 7. The time t of a single period of the order-1 periodic solution with the growth rate r of phytoplankton.

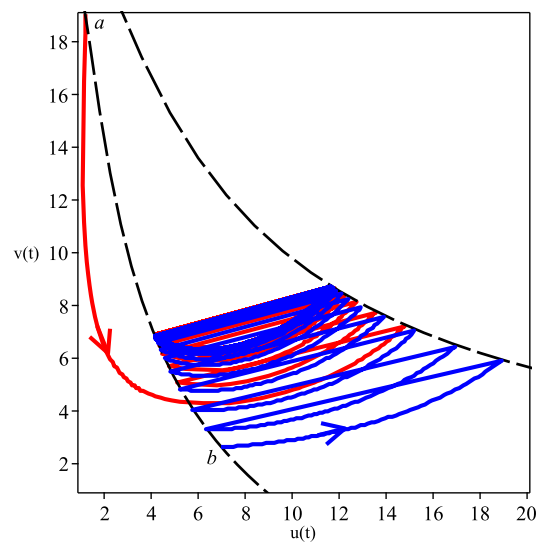


Figure 8. The path curve of system (2.3) starting from the points a and b .

6. Conclusions

In this paper, we propose an integrated control model that takes into account fish population densities and their current growth rates. The control form adopted is more in line with the development law of biological populations, so that fish can be harvested in time, and more economic benefits can be obtained. We delve into the complex dynamics of the model and illustrate the effect of dynamic thresholds on system dynamics. In this paper, the existence and stability of periodic solutions of order-1, and the existence of periodic solutions of order- k ($k \geq 1$) are proved. The correctness of the theoretical results was verified by numerical simulation, indicating that the phytoplankton and fish population densities can maintain periodic oscillations through effective control strategies, that is, the population size can be controlled within a stable range.

The results of this paper are an extension of literature [32], and we believe that the innovation of this model is as follows:

1) This paper employs dynamic thresholds determined by fish population density and current fish growth rate. Fixed thresholds are a special case of dynamic thresholds, which are extensions of fixed thresholds. For example, when $a_1 = 1$, $b_1 = 0$ in model (2.3), it is the case of a fixed threshold.

2) The dynamic properties of the model can be better investigated using the method of Poincaré map. The application of control methods and research methods make the model (2.3) have more complex dynamics than the literature [32] as Theorems 3.1 and 3.2.

Due to the synthesis of various factors affecting the development of the population, the control method adopted in this paper is more realistic, and the obtained research results have practical guiding significance. The analysis method proposed in this paper also has reference value in analyzing impulse models with complex phase sets or impulse sets.

Acknowledgements

The paper was supported by the National Natural Science Foundation of China (No. 11872335).

Conflict of interests

Declare that there no of interest regarding the publication of this paper.

References

1. Y. Wang, W. Jiang, H. Wang, Stability and global Hopf bifurcation in toxic phytoplankton zooplankton model with delay and selective harvesting, *Nonlinear Dyn.*, **73** (2013), 881–896. <https://doi.org/10.1007/s11071-013-0839-2>
2. M. P. Sissenwine, J. G. Shepherd, An alternative perspective on recruitment overfishing and biological reference points, *Can. J. Fish. Aquat. Sci.*, **44** (1987), 913–918. <https://doi.org/10.1139/f87-110>
3. S. A. Khamis, J. M. Tchuenche, M. Lukka, M. Heiloe, Dynamics of fisheries with prey reserve and harvesting, *Int. J. Comput. Math.*, **88** (2011), 1776–1802. <https://doi.org/10.1080/00207160.2010.527001>
4. M. R. Garvie, C. Trenchea, Predator-prey systems depend on a prey refuge, *J. Theor. Biol.*, **360** (2014), 271–278. <https://doi.org/10.1016/j.jtbi.2014.07.016>
5. W. Zheng, J. Sugie, Global asymptotic stability and equiasymptotic stability for a time-varying phytoplankton-zooplankton-fish system, *Nonlinear Anal. Real World Appl.*, **46** (2019), 116–136. <https://doi.org/10.1016/j.nonrwa.2018.09.015>
6. T. Yang, *Impulsive Control Theory*, Springer-Verlag, 2001. <https://doi.org/10.1007/3-540-47710-1>
7. S. Tang, Y. Xiao, R. A. Cheke, Multiple attractors of host-parasitoid models with integrated pest management strategies: Eradication, persistence and outbreak, *Theor. Popul. Biol.*, **73** (2008), 181–197. <https://doi.org/10.1016/j.tpb.2007.12.001>
8. L. Qian, Q. Lu, J. Bai, Z. Feng, Dynamics of a prey-dependent digestive model with state-dependent impulsive control, *Int. J. Bifurcation Chaos*, **22** (2012), 1250092–1250103. <https://doi.org/10.1142/S0218127412500927>
9. S. Sun, C. Guo, C. Qin, Dynamic behaviors of a modified predator-prey model with state-dependent impulsive effects, *Adv. Differ. Equations*, (2016), 1–13. <https://doi.org/10.1186/s13662-015-0735-9>
10. T. Ghiocel, Specific differential equations for generating pulse sequences, *Math. Prob. Eng.*, **2010** (2009), 242–256. <https://doi.org/10.1155/2010/324818>
11. T. Yuan, K. Sun, A. Kasperski, L. Chen, Nonlinear modelling and qualitative analysis of a real chemostat with pulse feeding, *Discrete Dyn. Nat. Soc.*, **2010** (2010), 179–186. <https://doi.org/10.1155/2010/640594>

12. X. Yu, S. Yuan, T. Zhang, Survival and ergodicity of a stochastic phytoplankton-zooplankton model with toxin-producing phytoplankton in an impulsive polluted environment, *Appl. Math. Comput.*, **347** (2019), 249–264. <https://doi.org/10.1016/j.amc.2018.11.005>
13. K. Sun, T. Zhang, Y. Tian, Dynamics analysis and control optimization of a pest management predator-prey model with an integrated control strategy, *Appl. Math. Comput.*, **292** (2017), 253–271. <https://doi.org/10.1016/j.amc.2016.07.046>
14. X. Jiang, R. Zhang, Z. She, Dynamics of a diffusive predator prey system with ratio-dependent functional response and time delay, *Int. J. Biomath.*, **13** (2020), 2050036. <https://doi.org/10.1142/S1793524520500369>
15. Y. Luo, L. Zhang, Z. Teng, T. Zheng, Stability and bifurcation for a stochastic differential algebraic Holling-II predator-prey model with nonlinear harvesting and delay, *Int. J. Biomath.*, **14** (2020), 2150019. <https://doi.org/10.1142/S1793524521500194>
16. G. Zeng, L. Chen, L. Sun, Existence of periodic solution of order one of planar impulsive autonomous system, *J. Comput. Appl. Math.*, **186** (2006), 466–481. <https://doi.org/10.1016/j.cam.2005.03.003>
17. L. Chen, K. Shimamoto, Emerging roles of molecular chaperones in plant innate immunity, *J. Gen. Plant Pathol.*, **77** (2011), 1–9. <https://doi.org/10.1007/s10327-010-0286-6>
18. G. Jiang, Q. Lu, Impulsive state feedback control of a predator-prey model, *J. Comput. Appl. Math.*, **200** (2007), 193–207. <https://doi.org/10.1016/j.cam.2005.12.013>
19. L. Nie, Z. Teng, L. Hu, J. Peng, Qualitative analysis of a modified Leslie-Gower and Holling-type II predator-prey model with state dependent impulsive effects, *Nonlinear Anal. Real World Appl.*, **11** (2019), 1364–1373. <https://doi.org/10.1016/j.nonrwa.2009.02.026>
20. X. Hou, J. Fu, H. Cheng, Sensitivity analysis of pesticide dose on predator-prey system with a prey refuge, *J. Appl. Anal. Comput.*, **12** (2022), 270–293. <https://doi.org/10.11948/20210153>
21. Z. Zheng, Y. Zhang, S. Jing, Nonlinear impulsive differential and integral inequalities with nonlocal jump conditions, *J. Inequalities Appl.*, **2018** (2018), 1–22. <https://doi.org/10.1186/s13660-018-1762-3>
22. P. Ghosh, J. F. Peters, Impulsive differential equation model in methanol poisoning detoxification, *J. Math. Chem.*, **58** (2020), 126–145. <https://doi.org/10.1007/s10910-019-01076-3>
23. Q. Liu, M. Zhang, L. Chen, State feedback impulsive therapy to SIS model of animal infectious diseases, *Phys. A Stat. Mech. Appl.*, **516** (2019), 222–232. <https://doi.org/10.1016/j.physa.2018.09.161>
24. Y. Tian, S. Tang, R. A. Cheke, Nonlinear state-dependent feedback control of a pest-natural enemy system, *Nonlinear Dyn.*, **94** (2018), 2243–2263. <https://doi.org/10.1007/s11071-018-4487-4>
25. M. U. Akhmet, On the general problem of stability for impulsive differential equations, *J. Math. Anal. Appl.*, **288** (2018), 182–196. <https://doi.org/10.1016/j.jmaa.2003.08.001>
26. J. Fu, X. Chun, M. Lei, Algebraic structure and poisson integral method of snake-like robot systems, *Front. Phys.*, **9** (2021), 643016. <https://doi.org/10.3389/fphy.2021.643016>
27. J. Fu, L. Zhang, S. Cao, C. Xiang, W. Zao, A symplectic algorithm for constrained hamiltonian systems, *Axioms*, **11** (2022), 217. <https://doi.org/10.3390/axioms11050217>

28. S. Cao, J. Fu, Symmetry theories for canonicalized equations of constrained Hamiltonian system, *Nonlinear Dyn.*, **92** (2018), 1947–1954. <https://doi.org/10.1007/s11071-018-4173-6>
29. C. Liu, P. Liu, Complex dynamics in a harvested nutrient-phytoplankton-zooplankton model with seasonality, *Math. Prob. Eng.*, **2014** (2014), 1–13. <https://doi.org/10.1155/2014/521917>
30. A. Sharma, A. Sharma, K. Agnihotri, Dynamical analysis of a harvesting model of phytoplankton-zooplankton interaction, *World Acad. Sci. Eng. Technol. Int. J. Math. Comput. Phys. Quant. Eng.*, **8** (2015), 1013–1018.
31. L. S. Chen, H. D. Cheng, Modeling of integrated pest control drives the rise of semi-continuous dynamical system theory (in Chinese), *Math. Model. Appl.*, **10** (2021), 1–16. <https://doi.org/10.19943/j.2095-3070.jmmia.2021.01.01>
32. D. Li, Y. Liu, H. Cheng, Dynamic complexity of a phytoplankton-fish model with the impulsive feedback control by means of Poincaré map, *Complexity*, **2020** (2020), 1–13. <https://doi.org/10.1155/2020/8974763>
33. S. Tang, B. Tang, A. Wang, Y. Xiao, Holling II predator-prey impulsive semi-dynamic model with complex Poincaré map, *Nonlinear Dyn.*, **81** (2015), 1575–1596. <https://doi.org/10.1007/s11071-015-2092-3>
34. Y. Tian, K. Sun, L. Chen, Geometric approach to the stability analysis of the periodic solution in a semi-continuous dynamic system, *Int. J. Biomath.*, **7** (2014), 157–163. <https://doi.org/10.1142/S1793524514500181>
35. P. Feketa, V. Klinshov, L. L. Cken, A survey on the modeling of hybrid behaviors: how to account for impulsive jumps properly, *Commun. Nonlinear Sci. Numer. Simul.*, **1** (2021), 105955. <https://doi.org/10.1016/j.cnsns.2021.105955>



AIMS Press

©2023 the Author(s), licensee AIMS Press. This is an open access article distributed under the terms of the Creative Commons Attribution License (<http://creativecommons.org/licenses/by/4.0>)